

Evidence for weak antilocalization in epitaxial graphene

Xiaosong Wu¹, Xuebin Li¹, Zhimin Song¹, Claire Berger^{1,2}, Walt A. de Heer¹

¹*School of Physics, Georgia Institute of Technology, Atlanta, GA 30332*

²*LEPES/CNRS, BP 166, 38042 Grenoble cedex6, France*

(Dated: December 2, 2024)

Transport in ultrathin graphite on silicon carbide is graphene-like and appears to be dominated by the electron-doped epitaxial graphene layer at the interface. Weak antilocalization in 2D samples manifests itself as a broad cusp-like depression in the longitudinal resistance for magnetic fields $10 \text{ mT} < B < 5 \text{ T}$. An extremely sharp weak-localization resistance peak at $B = 0$ is also observed. These features quantitatively agree with recent graphene weak-localization theory. Scattering contributions from charges in the substrate and from trigonal warping due to the graphite layer are tentatively identified. The Shubnikov-de Haas oscillations show an anomalous Berry's phase. Their small amplitudes may be related to graphene scattering processes.

PACS numbers: 72.15.Rn, 73.20.Fz, 73.50.-h

Ultrathin graphite layers that are epitaxially grown on single crystal silicon carbide have intriguing two-dimensional (2D) electronic properties [1, 2] that resemble those of isolated graphene sheets [3, 4, 5, 6, 7, 8, 9, 10, 11]. Mesoscopic Hall bars can be patterned with standard lithography methods. Previous studies of patterned quasi-1D structures reveal a graphene-like Berry's phase and Fermi velocity [2]. The data indicate that the transport is dominated by the epitaxial graphene (EG) layer at the interface which, due to the built-in electric field, is charged with an electron density $n = 3.4 \times 10^{12} \text{ cm}^{-2}$. The 10 or so layers above the interface are essentially uncharged and contribute little to the transport.

The graphene-like properties indicate that, like a hypothetical free-standing graphene sheet, the electronic structure of EG results from the massless Dirac equation (or the Weyl equation). Hence the band-structure consists of two independent valleys with opposite chirality, centered at \mathbf{K}_\pm of the hexagonal Brillouin zone. For a normal 2D electron gas elastic backscattering is enhanced due to constructive quantum interference thereby increasing the resistance. A magnetic field suppresses the interference and hence reduces the resistance, giving rise to a negative magneto-resistance (MR). This phenomenon is called weak-localization (WL). In graphene however, this interference can be destructive so that backscattering is reduced rather than enhanced. A magnetic field suppresses this effect as well giving rise to a positive MR. This effect is called weak-anti-localization (WAL), which, in graphene, is related to the chirality of the quasiparticles [12]. Note that this effect is expected for graphene but not for graphite.

Depending on the relative magnitude of the intervalley scattering time τ_{iv} and the phase coherence time τ_ϕ , either WL or WAL has been predicted [13]. The phase interference correction to the resistance depends on the nature of the disorder [14, 15, 16, 17, 18]. Intervalley scattering, which breaks isospin symmetry, causes WL while valley symmetry conserving (SC) elastic scattering

causes WAL. Furthermore, McCann *et al.* [16], point out that the warping term in the Hamiltonian, which breaks the isotropic symmetry of the valleys, suppresses WAL.

For epitaxial graphene samples, electronic scattering from remote counter-ions in the substrate are of the SC type and cause WAL. On the other hand, scattering by atomically sharp disorder (*i.e.* local defects and edges) is an isospin symmetry breaking mechanism and gives rise to WL. Trigonal warping, which may be caused by the interlayer interactions of a graphene sheet on top of the EG layer, tends to suppress WAL. Hence scattering from each of the three components of the EG system is expected to contribute to the MR.

In the case that SC scattering dominates, the sheet magnetoresistance can be expressed as [16]:

$$\Delta\rho(B) = -\frac{e^2\rho^2}{\pi h} \left[F\left(\frac{2\tau_\phi}{\tau_B}\right) - F\left(\frac{2}{\tau_B(\tau_\phi^{-1} + \tau_{iv}^{-1})}\right) - 2F\left(\frac{2}{\tau_B(\tau_\phi^{-1} + \tau_{iv}^{-1} + \tau_w^{-1})}\right) \right] \quad (1)$$

$$F(z) = \ln z + \Psi\left(\frac{1}{2} + \frac{1}{z}\right).$$

In contrast, the magnetoresistance in conventional 2D metals due to the weak-localization is given by [19]:

$$\Delta\rho(B) = -\frac{2e^2\rho^2}{\pi h} \left[F\left(\frac{2\tau_\phi}{\tau_B}\right) - F\left(\frac{2\tau}{\tau_B}\right) \right]. \quad (2)$$

Here Ψ are the digamma functions, τ is the transport time [16], τ_w is the warping-induced relaxation time, $\tau_B = \hbar/2eDB$, where D is the diffusion constant. Eq. (1) shows that the amplitude of the WL peak at $B = 0$ depends on τ_{iv} . Another important implication is that WAL can manifest itself in relatively high magnetic fields (*i.e.* where mainly short return trajectories contribute to

the interference correction), even in the presence of significant intervalley scattering. Qualitatively, in that case the long tail of the negative MR will ultimately give way to a positive MR at high fields. In other words, the MR will have a sharp peak at $B = 0$ and a positive slope at higher fields. All of these interference corrections to the resistance diminish with increasing temperature due to the reduction of the phase coherence time.

An earlier study of a quasi-1D EG ribbon shows a high mobility and a long coherence length [2]. In that case, edge scattering was shown to dominate the electron transport. Also a sharp MR peak near $B = 0$, consistent with 1D WL, was observed. This is consistent with intervalley scattering from the graphene edges which is favorable for producing a WL peak.

In this Letter we report evidence for WAL in 2D EG. Due to the epitaxial growth, the EG layer is of high crystalline quality [20] and protected from the environment by the graphite layer. Ultra-thin graphite layers were made by thermal decomposition of single-crystal silicon carbide. Graphite layers were patterned to produce a standard Hall bar $100 \mu\text{m} \times 1000 \mu\text{m}$ in size. The wired samples were placed into a He⁴ cryostat providing temperatures down to 1.4 K. Standard four-point measurements were carried out using a lock-in. A magnetic field was applied perpendicular to the graphene layer. Applying a magnetic field parallel to the graphene layer diminished the magnetoresistance to 1.5 % of its perpendicular-field value. This establishes an upper limit to the angular dispersion of the normal EG layer of $\delta\theta \leq 0.015$. A detailed analysis on the WL peak in a perpendicular and parallel magnetic fields gives a lower upper limit : $\delta\theta \leq 0.006$. The transport electron density $3.8 \times 10^{12} \text{ cm}^{-2}$ was determined from the Shubnikov-de Haas (SdH) oscillations. The low field Hall slope is $137 \Omega/\text{T}$, corresponding to a Hall electron density of $n_H = 4.6 \times 10^{12} \text{ cm}^{-2}$, which agrees with the density from SdH oscillations.

In contrast to 1D samples, in 2D films, edge scattering is significantly reduced and universal conductance fluctuation are absent. The WL is strongly suppressed and a positive MR in the intermediate field region is observed. These properties are reflected in the model developed by McCann *et al.* (Eq. (1)).

We have studied two samples and both displayed similar behavior. Fig. 1 shows the low-field resistance ($|B| < 35 \text{ mT}$) of one sample for temperatures ranging from 1.4 K to 50 K, which consist of a temperature dependent peak around zero field and a temperature independent parabolic component. As conventional, to bring out the temperature dependent part of the MR, the 50 K data (for which the peak is absent) is subtracted from the lower temperature data $R^*(B, T) = R(B, T) - R(B, 50\text{K})$ and then the temperature dependent MR is calculated by $\Delta R^* = R^*(B, T) - R^*(0, T)$. An extremely sharp WL peak at $B = 0$ (upper-right inset of Fig. 2) indicates a

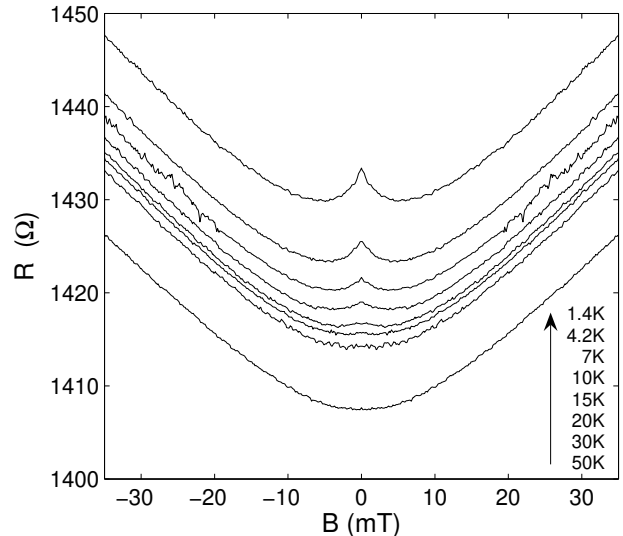


FIG. 1: Symmetrized low-field magnetoresistance for a sample of $100 \mu\text{m} \times 1000 \mu\text{m}$ at various temperatures. The electron mobility is $11600 \text{ cm}^2/\text{V}\cdot\text{s}$. The transport time $\tau \sim 0.26 \text{ ps}$ is inferred from the resistivity.

long phase coherence length (see below). As expected, the amplitude of the WL peak decreases while its width increases with increasing temperature as a result of the reduction of the phase coherence length. An attempt to fit the WL peak using conventional WL theory is shown in Fig. 2. Here a scaling factor $\alpha \sim 0.3$ was be introduced to obtain a reasonable fit about $B = 0$. This factor suggests that the WL is suppressed [22].

However an important deviation in ΔR^* from conventional WL theory is observed at fields above 20 mT where ΔR^* increases with increasing field up to $B = 4 \text{ T}$. This temperature dependent positive MR is a clear signature of WAL as discussed above. Moreover, the entire MR behavior is described very well by Eq. (1). Both the high field behavior of the MR, which is dominated by WAL for $B > 20 \text{ mT}$, and the low field behavior, for $B < 20 \text{ mT}$ which is dominated by WL [16], are convincingly reproduced (the fits are shown in Fig. 2 and the left inset). To produce this fit we reasonably assumed that τ_{iv} and τ_w are temperature independent, while τ_ϕ is temperature dependent. We find that τ_{iv} and τ_w are 1.0 ps and 0.28 ps, respectively. The temperature dependence of the phase coherence time τ_ϕ is plotted in Fig. 3. The coherence time is proportional to the inverse temperature, which, in 2D, is an indication that the dominant phase-breaking mechanism is *e-e* scattering. This is consistent with our previous results [2] and provides additional support for Eq. (1). (The deviation from linearity at the lowest temperature suggests a saturation of the coherence time. This is seen not only in our samples [2] but in 2D electron gases in general [21]. There is still no consensus on its origin.) To the best of our knowledge this constitutes the first experimental evi-

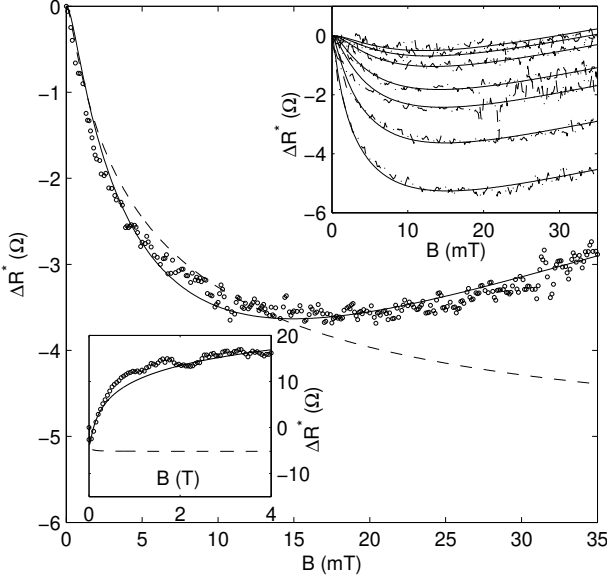


FIG. 2: Fit of low-field ΔR^* at 4.2 K to two models. ΔR^* is the magnetoresistance after subtracting a background as described in the main text. Open circles are the data. Dashed line is a fit to the WL theory for a normal 2D metal (Eq. (2)). A scaling factor $\alpha \sim 0.3$ is introduced in order to fit data, nevertheless an acceptable fit can only be obtained below 20 mT. Solid line is a fit to the model by McCann *et al.* (Eq. (1)). The fit shows a good agreement for the entire range of field. Right inset: dash-dot, ΔR^* for $T = 1.4$ K, 4.2 K, 7 K, 10 K, 15 K, 20 K, 30 K from bottom to top, solid line, fits to Eq. (1). Left inset: plot of the main panel extended to 4 T.

dence for WAL in graphene [23]. We stress that graphite shows normal WL [22] so that the WAL relates to the epitaxial graphene layer.

The temperature dependence of the e - e scattering time can be expressed as [24]:

$$\tau_{ee} = -\frac{2E_F\tau}{k_B \ln(T/T_1)} \cdot \frac{1}{T} \quad (3)$$

where E_F is the fermi energy, $k_B T_1 = \hbar^3 D^3 \kappa^4 \epsilon^2 / e^4$, ϵ and κ are the dielectric constant and screening constant, respectively. At low temperatures, the $\ln T$ dependence is usually negligible and $\tau_{ee} \simeq C/T$. The screening constant in 2D is given by $\kappa = 8\pi N e^2 / \epsilon$, where N is the density of states per spin per valley. For graphene, $N = k_F/hv_F$ and $\epsilon \approx 3.28$. So, we estimated $\kappa \approx 9.2 \times 10^6 \text{ cm}^{-1}$. We find that $T_1 \approx 2.7 \times 10^{10} \text{ K}$ so that $C \approx 63 \text{ ps}\cdot\text{K}$, which is of the same order as the value of 20 ps·K obtained from the plot in Fig. 3. Considering the complexity of Eq. (3), this is a remarkable agreement, which, again, supports the fit to Eq. (1).

Apparently SC scattering is the dominant elastic scattering mechanism in 2D epitaxial graphene giving rise to the extended WAL depression. Electronic scattering is likely to be caused by the long-range interactions with the counter-ions (“holes”) in the substrate. Note that the

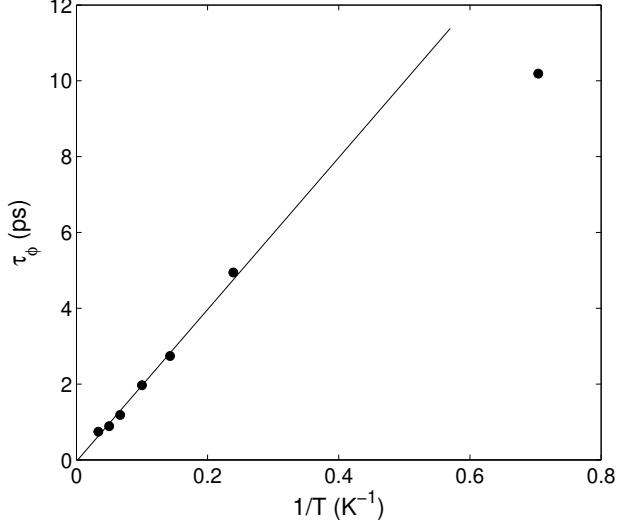


FIG. 3: Phase coherence time τ_ϕ as a function of inverse temperature $1/T$. τ_ϕ is obtained by a best fit to Eq. (1) for each temperature while τ_{iv} and τ_w are the same for all temperatures. Solid line is a guide to the eye.

electrons in the graphene and the holes in the substrate are a necessary consequence of the built in electric field at the interface of these dissimilar materials. Counter-ions in atomically flat, crystalline substrate should be uniformly distributed (more precisely the holes are delocalized), nevertheless, apparently residual inhomogeneities cause scattering. In this context, note that the semi-insulating 4H SiC material used in these experiments is lightly doped to pin the Fermi level in the middle of the gap. These impurities might contribute to the scattering.

The isospin symmetry breaking, intervalley scattering events are apparently relatively rare (*i.e.* scattering times are long), since WL effects are only observed at weak fields indicating that only long return trajectories involve such a scattering events. This is consistent with the high crystalline purity and the absence of edges in the 2D material. In contrast, in 1D samples edge scattering dominates. On the other hand, it should be expected that the SC scattering becomes ineffective in quasi-1D ribbons [12], (which is why carbon nanotubes tend to be ballistic conductors [25]). In fact we were not able to detect WAL in 1D ribbons (*e.g.* Ref. [2]).

After subtracting a quadratic background, extremely small but well-defined SdH oscillations (less than 0.2%) are observed in the high field resistance at 4.2 K (insets of Fig. 4). The Landau plot for the SdH oscillations (Fig. 4) shows a linear trend yielding a magnetic frequency $B_0 = 39 \text{ T}$. The almost zero intercept on the n axis indicates a Berry phase of π , consistent with graphene (see also Ref. [2]). In this case, the small amplitude of SdH oscillations cannot be caused by a short scattering time τ because $\tau \sim 0.26 \text{ ps}$, is longer than those in Ref. [4], where SdH oscillations even evolved into a quantum Hall

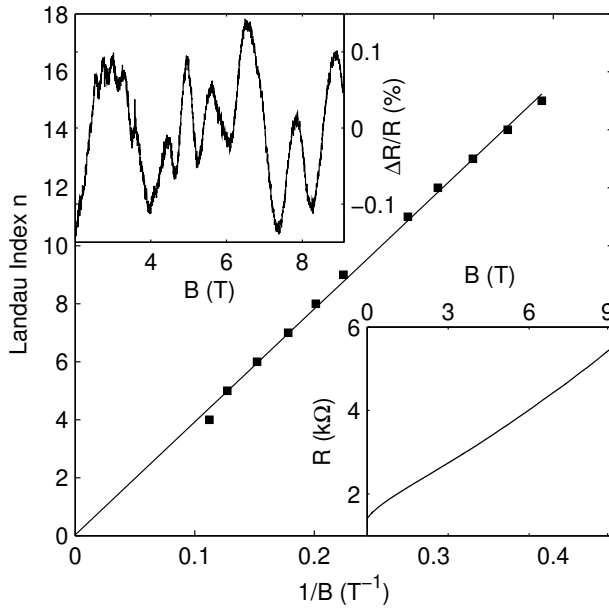


FIG. 4: Landau plot (Landau index n vs $1/B$) of the peaks of the SdH oscillations up to 9 T at 4.2 K (solid square). The solid line corresponds to a linear fit, which gives a magnetic frequency of 39 T and an intercept of 0.03 on the n axis, indicating the anomalous Berry's phase. Right inset: resistance as a function of the magnetic field at $T = 4.2$ K. Left inset: small SdH oscillations revealed after subtracting a quadratic background from the measured resistance that is plotted in the right inset.

effect. More striking is that the SdH amplitudes in 2D samples are much smaller than the SdH amplitudes in 1D samples (*c.f.* Ref. [2]). We find that the amplitudes are approximately inversely proportional to the sample width. This observation leads to the interesting speculation that in graphene scattering from atomically sharp defects enhances the SdH oscillation amplitudes, and consequently, that such local defects are also required to produce the integer quantum Hall effect. Apparently in our 2D samples the defect density of intervalley scatterers in the bulk is too low to produce large SdH oscillations or an integer quantum Hall effect.

In summary, epitaxial graphene exhibits a number of graphene properties. The isospin degeneracy that causes both weak antilocalization as well as the anomalous Berry's phase is a graphene property that is not present in graphite. It appears that the 2D bulk scattering in EG causes WAL and is dominated by valley symmetry conserving processes, consistent with scattering from long range potentials arising from charges in the substrate. WL appears to be primarily caused by isospin symmetry breaking scattering, for example from edges. Trigonal warping scattering due to the graphite layer on top of the EG could explain the reduction of the WAL. The extremely small SdH amplitudes (which preclude the QHE) may be directly related to the scattering processes

in the 2D bulk EG.

Supported by NSF grant 0404084, U.S. Department of Energy grant DE-FG02-02ER45956, a grant from Intel Research Corporation, and a USA-France travel grant from CNRS.

-
- [1] C. Berger *et al.*, *J. Phys. Chem. B* **108**, 19912 (2004).
[2] C. Berger *et al.*, *Science* **312**, 1191 (2006).
[3] K. S. Novoselov *et al.*, *Science* **306**, 666 (2004).
[4] K. S. Novoselov *et al.*, *Nature* **438**, 197 (2005); Y. B. Zhang *et al.*, *Nature* **438**, 201 (2005).
[5] Y. Zhang *et al.*, *Phys. Rev. Lett.* **96**, 136806 (2006).
[6] V. P. Gusynin and S. G. Sharapov, *Phys. Rev. Lett.* **95**, 146801 (2005).
[7] C. L. Kane and E. J. Mele, *Phys. Rev. Lett.* **95**, 226801 (2005).
[8] N. M. R. Peres, F. Guinea, and A. H. Castro Neto, *Phys. Rev. B* **73**, 125411 (2006).
[9] D. A. Abanin, P. A. Lee, and L. S. Levitov, *Phys. Rev. Lett.* **96**, 176803 (2006).
[10] K. Nomura and A. H. MacDonald, *Phys. Rev. Lett.* **96**, 256602 (2006).
[11] V. M. Pereira *et al.*, *Phys. Rev. Lett.* **96**, 036801 (2006).
[12] T. Ando and T. Nakanishi, *J. Phys. Soc. Jpn.* **67**, 1704 (1998).
[13] H. Suzuura and T. Ando, *Phys. Rev. Lett.* **89**, 266603 (2002).
[14] A. F. Morpurgo and F. Guinea, [cond-mat/0603789](http://arxiv.org/abs/cond-mat/0603789).
[15] D. V. Khveshchenko, *Phys. Rev. Lett.* **97**, 036802 (2006).
[16] E. McCann *et al.*, *Phys. Rev. Lett.* **97**, 146805 (2006).
[17] I. Aleiner and K. Efetov, [cond-mat/0607200](http://arxiv.org/abs/cond-mat/0607200).
[18] K. Nomura and A. MacDonald, [cond-mat/0606589](http://arxiv.org/abs/cond-mat/0606589).
[19] C. W. J. Beenakker and H. V. Houten, *Solid State Phys.* **44**, 1 (1991); B. L. Altshuler *et al.*, *Phys. Rev. B* **22**, 5142 (1980).
[20] J. Hass *et al.*, *Appl. Phys. Lett.* **89**, 143106 (2006).
[21] J. J. Lin and J. P. Bird, *J. Phys.: Condens. Matter* **14**, R501 (2002).
[22] S. V. Morozov *et al.*, *Phys. Rev. Lett.* **97**, 016801 (2006).
[23] A strong suppression of WL in graphene deposited on a SiO₂ substrate has recently been reported by Morozov *et al.* and attributed to corrugations of graphene sheets, which shift \mathbf{K}_\pm points. The shift ΔK is equivalent to a time reversal symmetry breaking gauge field, which suppresses WL. This curvature induced shift has been well studied in carbon nanotubes (Phys. Rev. Lett. **78**, 1932 (1997)). For a graphene sheet with a curvature radius of R , $\Delta K = a_0/16R^2$, where a_0 is the bond length. For graphene: $v_F = 3a_0\gamma_0/2\hbar$, Hence $\Delta K = \frac{3}{32} \frac{\gamma_0(a_0/R)^2}{\hbar v_F}$. It is the same formula used by Morozov *et al.* where a_0/R is replaced by ∇Z . For a sample with a height fluctuation of order h over a length d , $R \sim d^2/8h$, the gauge field $A = \hbar\Delta K/e = 4\hbar a_0 h^2/ed^4$. The flux through the ripple $\Phi = \oint \mathbf{A} \cdot d\mathbf{l}$. This results in $\Phi/\Phi_0 \sim 2a_0 h^2/d^3$, where Φ_0 is the flux quantum. In our sample, the angular dispersion of the normal to the graphene is 0.006. Even if $d \approx a_0$, the flux resulting from the distortion is $\Phi/\Phi_0 \sim 10^{-5}$, which produces a WL effect that is orders of magnitude to small to explain our data.

- [24] E. Abrahams *et al.*, Phys. Rev. B **24**, 6783 (1981); H. Fukuyama and E. Abrahams, Phys. Rev. B **27**, 5976 (1983).
- [25] S. Frank *et al.*, Science **280**, 1744 (1998).